http://ansinet.com/itj

ITJ

ISSN 1812-5638

INFORMATION TECHNOLOGY JOURNAL

ANSInet
Asian Network for Scientific Information
308 Lasani Town, Sargodha Road, Faisalabad - Pakistan

Information Technology Journal 12 (13): 2554-2560, 2013
ISSN 1812-5638 / DOI: 10.3923/itj.2013.2554.2560

3-D Calibration Algorithm for Freehand Ultrasound Image

[1]Yao Rao, [1]Lu Wenhua, [1]Zhang Xingyuan and [2]Yao Peng
[1]Aeronautic College, Shanghai University of Engineering Science, China
[2]School of Economics and Management, Beihua University, China

Abstract: 3-D calibration for freehand Ultrasound (US) image is an extremely important technique to build up 3-D US image system in ultrasound Non-destructive Testing (NDT). Calibration is a procedure to calculate the spatial transformation matrix, spatial relationship between the US image plane and the tracker attached to the US probe. In this research, a different cross-string phantom and the corresponding algorithm are investigated. The strings and crosses out of the scanning plane in the phantom accelerate interactive operation speed, guiding the operator to find the scanning plane quickly. Furthermore the ten crosses in the scanning plane provide the coordinates and spatial vectors for the calibration algorithm, thus the different calibration algorithm based on the least-squares fitting method of the homologous points matching can be realized. The results show that the US probe positioning time is no more than 5 sec. The precision and the accuracy results show that the algorithm calculates more accurate calibration matrix than that is obtained through the other published methods in the same operating time. The results solve the obligatory pre-procedure for computerize 3-D freehand ultrasonic in NDT.

Key words: Ultrasound image calibration, image processing, homologous points matching, non-destructive testing

INTRODUCTION

In ultrasound Non-destructive Testing (NDT), to computerize reconstruct the three-dimensional (3-D) model of the default in the US image, calibration for Ultrasound (US) image is an obligatory procedure. When operators apply the US probe to freehand scan an object, they obtain the non-parallel and irregular two-dimensional (2-D) ultrasound images sequence. Current reconstruction algorithms and tookits, such as VTK (Visualization ToolKit), are all developed based on the regular parallel image sequences. So these 2-D ultrasound images should be transformed into 3-D space, then interpolate the lost pixel if they are necessary, ultimately the regular and parallel image sequences be extracted. Then the 3-D reconstruction tookit will be feasible on tumor 3-D reconstruction. The above mathematical transformation procedure for 2-D coordinates of pixels in the US image to 3-D coordinates is the US image 3-D calibration. The US image 3D calibration is a procedure to calculate the transformation matrix between the US image and the tracker attached to the US probe. The transformation cannot be physically measured, only can be shown by a 4×4 matrix (rotation, translation and scale) through calibration.

The phantom structure design, the operation and algorithm speed and the precision and accuracy are three important factors to be considered when evaluate the US calibration (Mercier *et al*., 2005). What the calibration method initially proposed by Detmer applied a point target and iterative least-squares fitting method to calibrate the transformation matrix. This single point calibration method showed good results but it was time-consuming due to collecting procedure for a large number of US images. Since then the calibration techniques on the phantom investigation, the operating and algorithm speed acceleration and the precision improvement were researched persistently. Such as the operating and algorithm speed acceleration, researchers have mainly focused on the solid model given the special geometric characteristics during design. It is commonly be called phantom. This kind of phantom can reduce the operating and calculating time and reduce the errors caused by US probe alignment.

So in the last decade, to simplify the interaction and reduce the time, several phantoms and algorithms were researched (Prager *et al*., 1998; Blackall *et al*., 2000; Pagoulatos *et al*., 2001; Leotta, 2004; Dandekar *et al*., 2005; Hsu *et al*., 2008a). Abeysekera and Rohling (2011), De Lorenzo *et al*. (2011) and Melvaer *et al*. (2012) successively investigated their own optimized methods for phantoms and corresponding algorithms. To accelerate the calibration speed, the real-time 3-D US calibration methods were reported (Poon and Rohling, 2005; Hartov *et al*., 2010; Hsu *et al*., 2008b; Chen *et al*., 2009, 2011; Feng *et al*., 2012; Shao *et al*., 2012).

Corresponding Author: Yao Rao, Aeronautic College, Shanghai University of Engineering Science, China

In this research, a cross-string phantom was investigated to accelerate the calibration speed in the interaction operations procedure. More importantly, the different calibration algorithm based on the space vector was researched, which can optimize the least-squares fitting algorithm to calculate the more accurate calibration matrix than that is obtained through the past other ways in the same time.

CALIBRATION METHOD

Theory of calibration algorithm: The calibration is a procedure to find the spatial transformation relationships between the US image coordinate system and the tracking device coordinate system $T_{r\leftarrow i}$. Current tracking sensors mainly include the magnetic tracker and the optical tracker. In this research the magnetic tracker was selected which was also called magnetic receiver, receiver for short.

The whole coordinate definition and transformation relationships of the calibration system are shown in Fig. 1. Oi is the image coordinate system (this study defined). Or is the magnetic receiver coordinate system (magnetic manufacturer defined). Ot is the magnetic transmitter coordinate system (magnetic manufacturer defined, as the 3-D spatial coordinate system in this study). And the $T_{t\leftarrow r}$ is the transformation matrix that is the magnetic receiver coordinate system Or relative to magnetic transmitter coordinate system Ot. It is known from the algorithm of the magnetic tracking system. If an imaging pixel in the US image is marked as $P_i = [S_h \cdot x_i \; S_v \cdot y_i \; 0 \; 1]^T$, S_h, S_v are the image coefficients of the horizontal and the vertical directions (scales, mm/pixel), in general, $S_h = S_v$. it can be transferred into the 3-D coordinate system Ot and be marked as $P_i = [x_i \; y_t \; 0 \; 1]^T$. The transfer relationship is as Eq. 1:

$$\begin{pmatrix} x_t \\ y_t \\ z_t \\ 1 \end{pmatrix} = T_{t\leftarrow r} \cdot T_{r\leftarrow i} \cdot \begin{pmatrix} s_u \cdot x_i \\ s_v \cdot y_i \\ 0 \\ 1 \end{pmatrix} \quad (1)$$

Therefore, $T_{r\leftarrow i}$ is the research focus and generally is calculated through a phantom with special geometric characteristics as is shown in Fig. 1. Where Op is the phantom coordinate system (this study defined). The calibration target is calculating the transformation matrix $T_{r\leftarrow i}$ between the Oi and Or through the assistant coordinate systems Ot and Op. When the US probe is

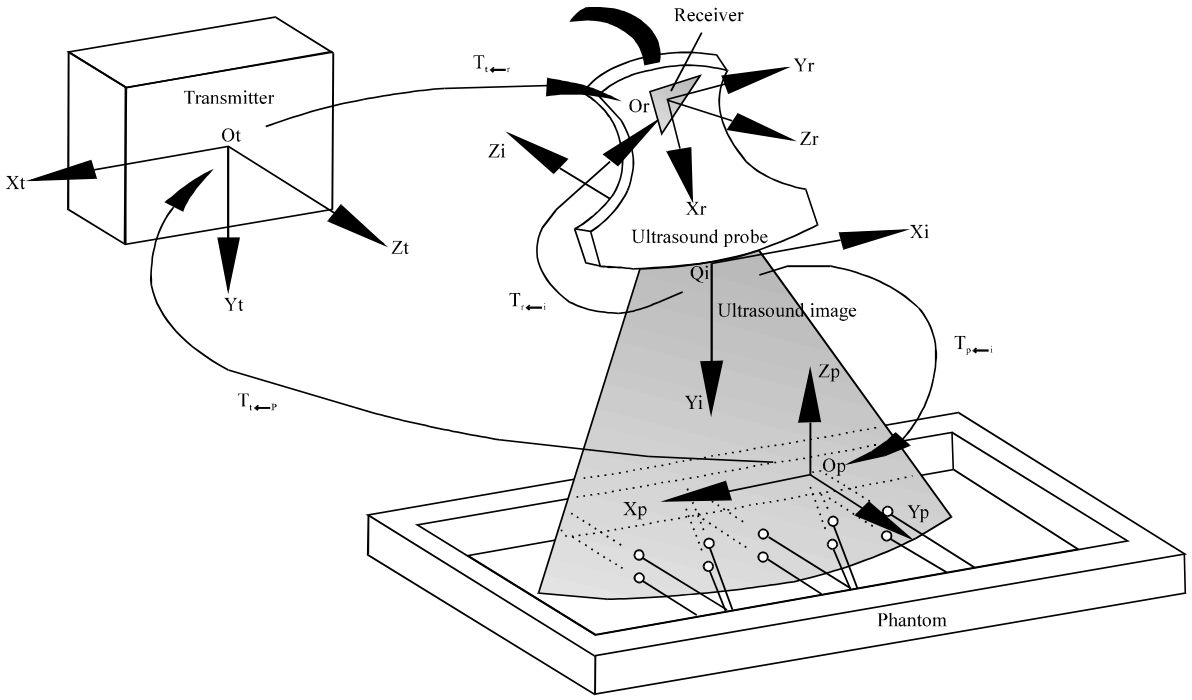

Fig. 1: Coordinate systems definition and transformation relationships include receiver transmitter, receiver, phantom and image coordinate systems

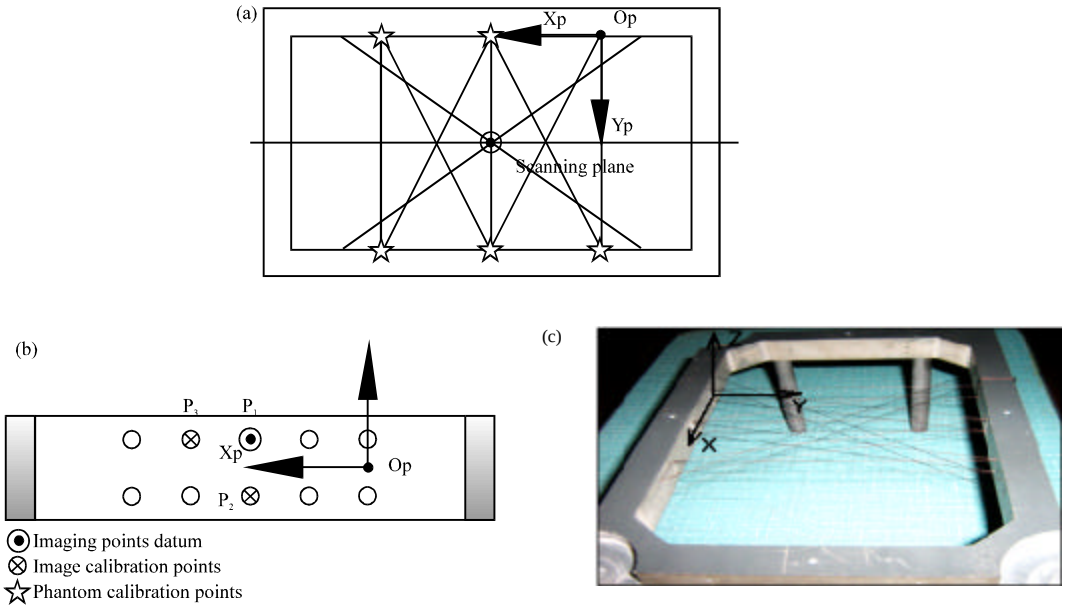

Fig. 2(a-c): Phantom construction and coordinate systems definition, (a) Phantom top view, (b) Scanning plane view and algorithm points and (c) Phantom photo

placed upon the phantom as seen in Fig. 1, if a point in the phantom is marked as $P_p = [x_p\ y_p\ 0\ 1]^T$. The coordinate transformation matrix between Op and Oi is:

$$\begin{pmatrix} x_p \\ y_p \\ z_p \\ 1 \end{pmatrix} = T_{p\leftarrow t} \cdot T_{t\leftarrow r} \cdot T_{r\leftarrow i} \cdot \begin{pmatrix} s_h \cdot x_i \\ s_v \cdot y_i \\ 0 \\ 1 \end{pmatrix} \quad (2)$$

Shortening:

$$P_p = T_{p\leftarrow t} \cdot T_{t\leftarrow r} \cdot T_{r\leftarrow i} P_i \quad (3)$$

where, $T_{p\leftarrow t}$ is the transformation matrix between the magnetic transmitter coordinate system Ot and the phantom coordinate system Op. It is calculated by the algorithm in this study. Equation 4 is only by matrix expression:

$$T_{p\leftarrow i} = T_{p\leftarrow t} \cdot T_{t\leftarrow r} \cdot T_{r\leftarrow i} \quad (4)$$

Finally the image calibration $T_{r\leftarrow i}$ in matrix:

$$T_{r\leftarrow i} = T_{t\leftarrow r}^{-1} \cdot T_{p\leftarrow t}^{-1}\ T_{p\leftarrow i} \quad (5)$$

Phantom and $T_{p\leftarrow t}$ calibration: Therefore, in order to obtain $T_{r\leftarrow i}$, $T_{p\leftarrow t}$ must be acquired firstly. As is presented in Fig. 2. cross-string phantom is consisted of cross-string, their planar arrays and phantom frame. The cotton strings of the cross-string are 0.3 mm in diameter. Because of their elasticity, they can keep tightened to maintain the string's position precision both in dry and water conditions. The cotton stings pass through the holes, 1 mm in diameter, on both front and back walls and form two layers of cotton strings arrays.

The 10 endpoints (holes) of all the vertical strings in the two sides opposite are the marked points (Fig. 2). They are marked as the stars, double 2 endpoints in the up side and double 3 endpoints in the down side. All coordinates of the marked points in the phantom coordinate system P_p are given when the phantom is designed. Place the needle attached with the tracker (magnetic receiver) in the holes, through magnetic tracking algorithm $T_{t\leftarrow r}$, the coordinates of these holes in Ot (the magnetic transmitter coordinate system) are calculated, marked as P_t. Apply the least-square fitting to P_p and P_t:

$$\min_{R,p} \sum \left\| P_p - (RP_t + p) \right\|^2 \quad (6)$$

Through finding the minimized distance between the homologous points P_p and P_* the least-square fitting method calculate the transformation matrix $T_{p\leftarrow t} = (R, p)$. where, R is rotation and p is translation vector.

Imaging: After phantom calibration $T_{p\leftarrow t}$, place the US probe upon the cross-strings align with the middle string cross planar arrays (Fig. 3), adjust the probe's orientation

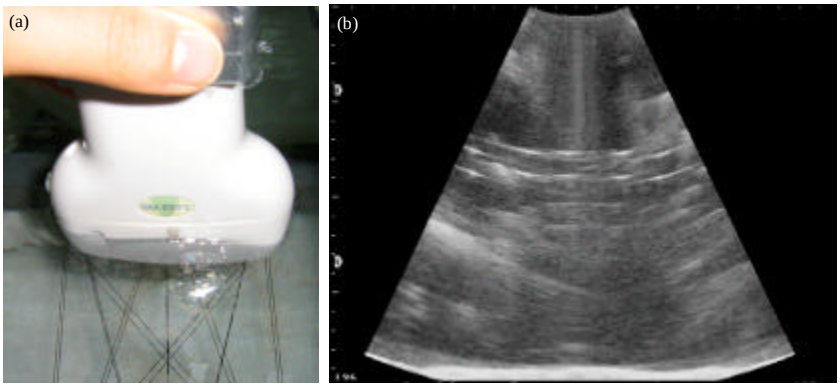

Fig. 3(a-b): Probe scanning and ultrasound imaging, (a) Place the probe upon the middle crosses planar of the strings in the phantom and (b) Ten lightened points in the US image

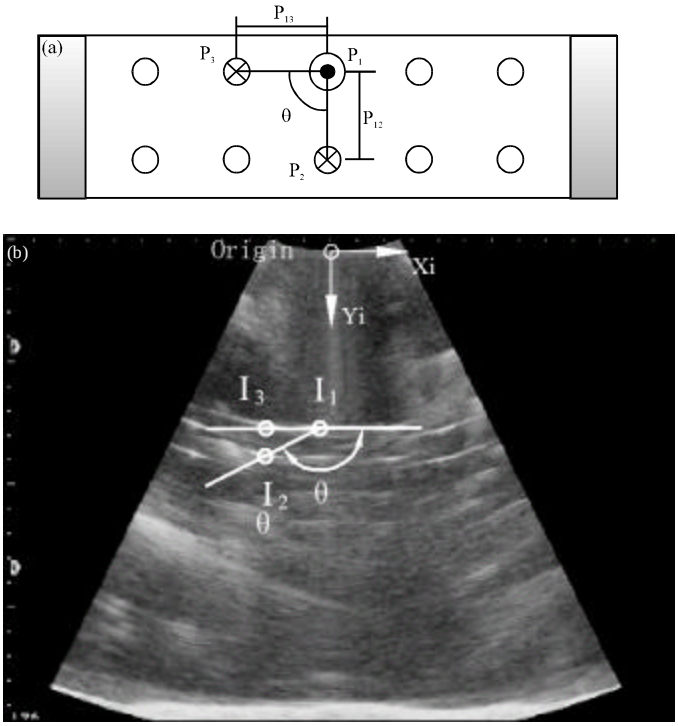

Fig. 4(a-b): Image calibration algorithm, (a) Homologous points and matching parameters in phantom and (b) Homologous points in image and algorithm

and position, to ensure the image plane make intersection with the cross-string layers. Until the 10 middle points are all in the US image, two layers, 5 imaging points in each layer, total 10 imaging points are shown. In this procedure, the strings trend nearby the middle cross arrays are help the probe find the middle cross arrays rapidly. The image origin is defined at the centre of the sector surface of the US image (Fig. 4).

Image calibration algorithm: The image calibration algorithm is as in the Fig. 4. There are ten imaging points in the scanning image. They are the corresponding images of the cotton strings crosses in the phantom. But only two points' coordinates are used in the calibration algorithm. They are I_1 and I_3 (Fig. 4b). The coordinates of P_1, P_2, P_3, d_{12} and d_{23} in the phantom are known by design, so the angle θ between $\overline{P_1P_3}$ and $\overline{P_1P_2}$ is calculated by P_1,

P_2 and P_3 (Fig. 4a). Then θ with the distances d_{12} and d_{23} provide three parameters for calculating the image point I_2 and I_3.

The calibration procedure is as followings:

- **Manual mark I_1:** I_1 is the middle point of the up layer of the ten points sequence in the scanning image. Select I_1 as the reference point, because it is nearby the centre line of the sector region in the US image. As the reference of the other points, the distances of other points' relative to it should be calculated. Its homologous point is the P_1 in the phantom, homologous point in the receiver $R_1 = T_{r\leftarrow t} \cdot T_{t\leftarrow p} \cdot P_1$
- **Manual mark and calculate I_2:** I_2 is a point near the middle point of the layer below of the ten points sequence in the scanning image. Firstly, marking the highlight point below the reference point I_1 to determine the direction of the vector $\overrightarrow{I_1I_2}$. Then calculating the distance from I_1 to I_2 according to d_{12} (be converted to pixel). The homologous point of I_3 is the P_2 in the phantom. So homologous point in the receiver is $R_2 = T_{r\leftarrow t} \cdot T_{t\leftarrow p} \cdot P_2$
- **Calculate I_3:** I_3 is a point near the reference point' left side along the vector $\overrightarrow{I_1I_3}$. The direction of $\overrightarrow{I_1I_3}$ is calculated by $\overrightarrow{I_1I_2}$ rotating an angle θ around I_1. And the distance from I_1 to I_3 can be calculated according to d_{13} (be converted to pixel). The homologous point of I_3 is the P_3 in the phantom. So homologous point in the receiver is $R_3 = T_{r\leftarrow t} \cdot T_{t\leftarrow p} \cdot P_3$
- Collect 4 US images and repeat 1-3
- Apply the least-square fitting to $P_r(R)$ and $P_i(I)$

$$\min_{R,p} \sum \left\| P_r - (sRP_i + p) \right\|^2 \tag{7}$$

where, s is the coefficients of the image (scales, mm/pixel). Calculate the transformation matrix $T_{r\leftarrow i} = (R, p)$ (R: rotation matrix, p: translation vector) by the theory of finding the minimized distance between the homologous points P_r and P_i [1]. $T_{r\leftarrow i}$ is shown as a 4×4 matrix (rotation, translation and scale) lile Eq. 8. Its first three columns form R and the fourth column forms p:

$$T_{r\leftarrow i} = \begin{bmatrix} P_{11} & P_{12} & P_{13} & P_{14} \\ P_{21} & P_{22} & P_{23} & P_{24} \\ P_{31} & P_{32} & P_{33} & P_{34} \\ 0 & 0 & 0 & 1 \end{bmatrix} \tag{8}$$

The calibration matrix can be calculated from a single US image. However, due to the variations when the probe is placed upon the phantom to find the scanning plane with freehand scanning mode, the final calibration matrix is calculated based on 4 images repeated the manual marking and coordinates calculation. Then use each mass center of the homologous points to calculate the transformation matrix. In each US image, the two imaging points are manual marked by this self-developed software.

EXPERIMENTS AND RESULTS

In this experiments, the devices are the ZK-3000 ultrasound equipment produced by Zhongke Tianli Ltd. in Beijing with the probe is 3.5/5.0 R60 and the AURORA magnetic tracker (attached to the probe) is from the NDI in Canada.

Calibration precision: The calibration precision can be evaluated by the discrete degree of the element in the calibration matrix. The major factors causes the variations of the elements of calibration are: (1) Positioning errors when the stylus being placed into the hole on the phantom during phantom calibration (stylus measurements), (2) Placement incorrect when the phantom scanned by probe with freehand (phantom imaging) and (3) Manual errors of the pixel coordinates of the crosses in the US image (manual image marking). In the past researches, the third aspect is the most difficult to decease the errors. This experiment method is, except for the method of homologous points in Fig. 4, select the points with different distances and angles to the reference point to calculate the matrix and average them as the final calibration matrix.

Repeat each of above three operations 10 times and computing variations of the calibration matrix. The probe was moved away from the strings and repositioned for each of the 4 images. This method ensures the independency of each image collection and presents the actual precision of the repeated calibration. The results are shown in Table 1. The first six rows are the rotation matrix elements and the last three rows are the translation vector in millimeters. The third column of calibration matrix is not shown, because it is the cross-product of the first two columns. The maximum discrete degrees (0.4024-0.6199 mm) are in the phantom imaging experiments. Compare this data with other past methods, such as 0.63-2.64 mm (Leotta, 2004), the calibration precision is improved.

Reconstruction accuracy: The repeated precision reflects the stability degree of the calibration matrix, but does not provide an estimate of the validity of the calibration matrix, the effect of its 3-D transformation, so the reconstruction accuracy evaluation is necessary. The method is: (1) Apply the calibration matrix to translate the ten points in each image into the 3-D coordinate system

Table 1: Precisians statistics of the calibration matrix elements

	Repeated phantom imaging (10 times)			Repeated manual image marking (10 times)			Repeated stylus measurements (10 times)		
Matrix elements	Mean	SD	Range	Mean	SD	Range	Mean	SD	Range
P_{11}	0.9527	0.0003	0.0009	0.9459	0.0001	0.0003	0.9566	0.0002	0.0007
P_{21}	-0.2970	0.0130	0.0491	-0.2907	0.0102	0.0305	-0.2897	0.0095	0.0179
P_{31}	-0.0640	0.0038	0.0126	-0.0589	0.0021	0.0084	-0.0622	0.0032	0.0101
P_{12}	0.0418	0.0063	0.0187	0.0462	0.0052	0.0103	0.0393	0.0041	0.0129
P_{22}	0.3369	0.0004	0.0012	0.3342	0.0003	0.0007	0.3304	0.0002	0.0005
P_{32}	-0.9406	0.0001	0.0003	-0.9413	0.0001	0.0003	-0.9396	0.0003	0.0008
P_{14}	-16.4161	0.2052	0.6199	-16.2809	0.0802	0.2316	-16.3069	0.0813	0.2546
P_{24}	-86.6574	0.1521	0.4593	-86.7937	0.0430	0.1269	-86.7312	0.0359	0.1090
P_{34}	-39.1202	0.1186	0.4024	-39.1586	0.0985	0.2936	-39.0577	0.1064	0.3102

Table 2: Comparison reconstruction results

Calibration source	Point target variability rms (mm)	Two points distance error (Mean±SD)
A	0.97	27.23±1.01
B	1.03	27.64±0.18
A1	0.98	27.81±0.67
A2	0.92	26.39±0.85
A3	0.98	27.76±0.34
A4	0.95	26.72±0.38
B1	1.06	26.85±1.04
B2	1.03	26.99±0.27
B3	0.91	26.93±0.27
B4	1.08	27.50±0.81

A: Middle 6 points reconstruction accuracy, B: Outer 4 points reconstruction accuracy

and then calculate the root mean square (rms), evaluating the stability of reconstruction. (2) Apply the calibration matrix to translate the three point, I_1, I_2 and I_3, calculate the distance between I_1 and I_2, I_1 and I_3, then compare the distances with the real distances in the phantom. These data reflect the relative reconstruction accuracy. The experiment was divided into two groups, A: repeat the above to two procedures using the middle 6 points to calculate the reconstruction accuracy and B: repeat the above to two procedures using the outer 4 points to calculate the reconstruction accuracy. The results as seen in Table 2 show that the reconstruction accuracy of the middles points is similar to that of the outer points. The 3-D reconstruction accuracy is about ±1 mm in both point target variability (repeated precision of reconstruction) and distance error (reconstruction accuracy). It is a relative high accuracy compare with other past researches.

CONCLUSION

This study investigates a different calibration method for freehand 3-D US system through cross-string phantom and corresponding calibration algorithm:

- The phantom was in cross cottons structure. The ten crosses in the scanning plane provided the coordinates and space vectors for the calibration algorithm and the crosses and the strings out of the scanning plane guided the probe to align with the scanning plane fast and accurately
- The space vectors and the angle between the two vectors were calculated based on the ten crosses coordinates, furthermore the homologous points in the US image and in the phantom were obtained, matching them through the least-squares fitting method to calculate the spatial transformation matrix between the US image and the tracking sensor attached to the US probe
- The operation results show that the scanning plane positioning time is no more than 5s, faster than other method. And the precision and accuracy results demonstrate that the algorithm calculates more accurate calibration matrix than that is obtained through the past reported methods in the same operating time

ACKNOWLEDGMENTS

This work was supported by National Natural Science Foundation of China (30825010), Key Projects of Beijing Science and Technology Committee (H060720050330) and Shaihai 12-5 Connotation Construction Project for University (B-8932-12-0131).

REFERENCES

Abeysekera, J.M. and R. Rohling, 2011. Alignment and calibration of dual ultrasound transducers using a wedge phantom. Ultrasound Med. Biol., 37: 271-279.

Blackall, J.M., D. Rueckert, C.R. Jr. Maurer, G.P. Penney, D.L.G. Hill and D.J. Hawkes, 2000. An Image Registration Approach to Automated Calibration for Freehand 3D Ultrasound. In: Medical Image Computing and Computer-Assisted Intervention, Delp, S.L., A.M. DiGoia and B. Jaramaz (Eds.). Springer, Pittsburgh, PA, pp: 462-471.

Chen T.K., A.D. Thurston, R.E. Ellis and P. Abolmaesumi, 2009. A real-time freehand ultrasound calibration system with automatic accuracy feedback and control. Ultrasound Med. Biol., 35: 79-93.

Chen, T.K., R.E. Ellis and P. Abolmaesumi, 2011. Abolmaesumi improvement of freehand ultrasound calibration accuracy using the elevation beamwidth profile. Ultrasound Med. Biol., 37: 1314-1326.

Dandekar, S., Y. Li, J. Molloy and J. Hossack, 2005. A phantom with reduced complexity for spatial 3-D ultrasound calibration. Ultrasound Med. Biol., 31: 1083-1093.

De Lorenzo, D., A. Vaccarella, G. Khreis, H. Moennich, G. Ferrigno and E. de Momi, 2011. Accurate calibration method for 3D freehand ultrasound probe using virtual plane. Med. Phys., 38: 6710-6720.

Feng, N., J. Liu, L. Ma and M. Sun, 2012. Ultrasound image deconvolution based on dynamic SNR estimation. Int. J. Adv. Comput. Technol., 4: 287-293.

Hartov, A., K. Paulsen, S. Ji, K. Fontaine, M.L. Furon, A. Borsic and D. Roberts, 2010. Adaptive spatial calibration of a 3D ultrasound system. Med. Phys., 37: 2121-2130.

Hsu, P., R. Prager, A. Gee and G.M. Treece, 2008a. Real-time freehand 3D ultrasound calibration. Ultrasound Med. Biol., 34: 239-251.

Hsu, P.W., G.M. Treece, R.W. Prager, N.E. Houghton and A.H. Gee, 2008b. Comparison of freehand 3-D ultrasound calibration techniques using a stylus. Ultrasound Med. Biol., 34: 1610-1621.

Leotta, D.F., 2004. An efficient calibration method for freehand 3-D ultrasound imaging systems. Ultrasound Med. Biol., 30: 999-1008.

Melvaer, E.L., K. Morken and E. Samset, 2012. A motion constrained cross-wire phantom for tracked 2D ultrasound calibration. Int. J. Comput. Assist. Radiol. Surg., 7: 611-620.

Mercier, L., T. Lango, F. Lindseth and D.L. Collins, 2005. A review of calibration techniques for freehand 3-D ultrasound systems. Ultrasound Med. Biol., 31: 143-165.

Pagoulatos, N., D.R. Haynor and Y. Kim, 2001. A fast calibration method for 3-D tracking of ultrasound images using a spatial localizer. Ultrasound Med. Biol., 27: 1219-1229.

Poon, T.C. and R.N. Rohling, 2005. Comparison of calibration methods for spatial tracking of a 3-D ultrasound probe. Ultrasound Med. Biol., 31: 1095-1108.

Prager, R.W., A. Gee and L. Berman, 1998. Stradx: Real-time acquisition and visualization of freehand three-dimensional ultrasound. Med. Image Anal., 3: 129-140.

Shao, D., P. Liu and D.C. Liu, 2012. Histogram-based fast adaptive bilateral filter for ultrasound speckle reduction. Int. J. Digital Content Technol. Applicat., 6: 298-305.